Photo-Acoustic Measurement of Thermal Conductivity of Thin Films and Bulk Materials

Xinwei Wang
Hanping Hu[1]
Xianfan Xu

School of Mechanical Engineering,
Purdue University,
West Lafayette, IN 47907

The photoacoustic (PA) technique is one of many techniques for measuring thermal conductivity of thin films. Compared with other techniques for thermal conductivity measurement, the photoacoustic method is relatively simple, yet is able to provide accurate thermal conductivity data for many types of thin films and bulk materials. In this work, the PA measurement in a high frequency range is made possible by a newly developed PA apparatus, which extends the limit of the PA technique. Thermal conductivities of SiO_2 with thicknesses from 0.05 to 0.5 μm on Si wafer, e-beam evaporated thin nickel film on Si wafer, and thermal barrier coatings are obtained. In addition to the commonly used phase shift fitting, which is only appropriate for thermally-thin films, an amplitude fitting method is developed and employed for measuring both thin films and bulk materials with smooth or rough surfaces. Comparing results by amplitude fitting to those obtained by other methods and reference values shows good agreements. Applications and limitations of the photoacoustic technique are discussed. [DOI: 10.1115/1.1337652]

Keywords: Contact Resistance, Heat Transfer, Measurement Techniques, Thermoacoustics, Thin Films

I Introduction

Thermal property data are important for any material that experiences heat transfer. The thermal conductivity and diffusivity of thin films are essential for the thin film manufacturing process, as well as for their applications in microelectronic devices. In devices such as radiation detectors, laser diodes, and transistors in electronic circuits, heat accumulated during device operation needs to be rapidly removed, which is greatly affected by their thermal conductivity and diffusivity.

It has been well known that the thermal conductivity of thin films may differ significantly from the bulk value due to the difference in microstructure such as the grain size, amorphousness, and concentration of foreign atoms and defects, which strongly affect the scattering process of the energy carriers. Although theories have been developed to predict the thermal conductivity of thin films, experiments are often needed to determine thermal conductivity of thin films owing to the complexity of the thin film microstructure. Since the microstructures of thin layers depend strongly on fabrication techniques, thermal conductivity measurements must be performed on the same microstructures fabricated with the same processes as those used in real devices for which the thermal conductivity is needed. In the last decade, many techniques have been developed to measure thermophysical properties of thin film materials. Goodson and Flik [1] reviewed techniques for measuring thermal conductivity along and across thin film layers. It is concluded that more detailed uncertainty analysis is required for most of the available techniques. More recently, Mirmira and Fletcher [2] reviewed experimental and analytical techniques for measuring and predicting thermal conductivity of thin films.

Techniques for thermal conductivity measurement can be categorized into contact and non-contact methods. In contact measurements, normally a thin metal film is deposited onto the sample surface that is subsequently patterned into electric circuitry. The temperature response of the sample structure under thermal loading is sensed by the circuit, and related to unknown thermal properties. Methods in this category include the bolometer method [3], 3ω and extended 3ω method [4–6], pulse heating method [7], and micro bridge method [8–10]. Drawbacks of the contact methods are that they are limited to dielectric thin films only, and the sample preparation process is laborious.

The other category of the thermal conductivity measurement technique is the non-contact method. Optical techniques belong to this category, for which the optical response of a probing beam is measured when the sample is subjected to photothermal excitation. The thermal conductivity of the sample can be obtained by measuring the phase shift of the reflected beam due to surface deformation [11], the reflectivity change due to pulse laser heating [10], or deflection of the probing beam due to change of the index of refraction of air near a heated sample [12]. For the reflectance measurement, pico and subpicosecond lasers have been used [13], which make it possible to measure thermal conductivities of thin films as thin as nanometers. In addition to the measurement of thermal properties, the picosecond pulse induced ultrasound was used to simultaneously determine the thickness of the thin film [14].

The photoacoustic (PA) method is a relatively simple, non-contact method for measuring thermal conductivities. However, this method has not received much attention for measuring thermal properties of thin films. For example, there is no discussion of this technique in the review papers mentioned above. In the PA measurement, a heating source, normally a laser beam, is periodically irradiated on the sample surface. The acoustic response of the air above the sample is measured and related to thermal properties of the sample. A review of the PA technique was given by Tam [15]. The PA phenomenon was first explained by Rosencwaig and Gersho [16] as the result of thermal expansion of the gas adjacent to the sample surface. An analytic solution of the PA response of a single layer on a substrate was also given by Rosencwaig and Gersho [16]. Since then, a number of detailed investigations have been performed. Fujii et al. [17] derived an analytical solution of the PA response of two layers of films on a substrate. Baumann and Tilgner [18] developed a model for cases of any number of layers. The constraints of their model are that

[1]On leave from the Department of Thermal Science and Energy Engineering, University of Science and Technology of China, China.

Contributed by the Heat Transfer Division for publication in the JOURNAL OF HEAT TRANSFER. Manuscript received by the Heat Transfer Division October 25, 1999; revision received, June 25, 2000. Associate Editor: A. Majumdar.

the laser beam has to be absorbed within the first layer, and no thermal contact resistance is considered. Cole and McGahan [19] provided a solution which can be used for more general PA problems, which considers optical absorption in any layer and contact resistances between layers of a multilayer system. Numerical integration is required to calculate the temperatures in films and in substrate. The PA technique has been used successfully to obtain thermal conductivity of thin films. By fitting amplitude and phase shift of PA signals, Lachaine and Poulet [20] measured the thermal conductivity of 18 μm-thick polyester films. Raman et al. [21] measured the thermal diffusivity by determining the frequency ascertaining whether a layer is thermally thin or thermally thick. By fitting the phase shift of the PA signal, Rohde [22] measured the thermal conductivity of films as thin as 500 nm.

In this work, a PA measurement apparatus is designed for measurements up to a frequency of 20 kHz, higher than the highest frequency used by other investigators (2 kHz). This allows properties of thinner films to be measured. Also an amplitude fitting method is developed to measure bulk materials or films with rough surfaces. The data reduction procedure is based on the recently developed generalized photoacoustic model [23]. By fitting phase shift and amplitude of PA signals, thermal conductivity data of thin SiO_2 films, thin nickel film, thermal barrier coatings, and bulk materials with smooth and rough surface are obtained.

II Theory of the Photoacoustic Method

The sample considered in this work consists of a backing material (0) and N successive layers $(1,2,\cdots,N)$, and is heated by a modulated laser beam with an intensity of $1/2\cdot I_0(1+\cos(\omega t))$. The coordinate x is originated from the surface of the sample and pointing outward. Absorption of the laser beam is allowed in any layer, and in more than one layer. An additional medium $(N+1)$, such as air, is in contact with the surface layer (N). The backing material (0) and the surrounding medium $(N+1)$ are considered to be thermally thick. It has been shown that when the thermal diffusion length in gas is much less than the radius of the sample chamber, the PA signal is independent of the energy distribution of the incident laser beam [24]. Therefore, a one-dimensional model of the PA effect is adequate. The transient temperature field in the multilayer sample and air can be derived by solving a set of one-dimensional heat conduction equations. Details of the derivation process have been described elsewhere [23]. The solution of the complex temperature distribution θ_{N+1} in the air can be expressed as

$$\theta_{N+1}=(1-\rho)\cdot B_{N+1}e^{-\sigma_{N+1}x}e^{j\omega t}, \tag{1}$$

where

$$B_{N+1}=-\frac{[0\ \ 1]\cdot\sum_{m=0}^{N}\left(\prod_{i=0}^{m-1}U_i\right)\cdot V_m\cdot\begin{bmatrix}E_m\\E_{m+1}\end{bmatrix}}{[0\ \ 1]\cdot\left(\prod_{i=0}^{N}U_i\right)\cdot\begin{bmatrix}0\\1\end{bmatrix}}; \tag{2}$$

$$U_i=\frac{1}{2}\begin{bmatrix}u_{11,i} & u_{12,i}\\ u_{21,i} & u_{22,i}\end{bmatrix};\quad V_i=\frac{1}{2}\begin{bmatrix}\nu_{11,i} & \nu_{12,i}\\ \nu_{21,i} & \nu_{22,i}\end{bmatrix}; \tag{3a}$$

$$u_{1n,i}=(1\pm k_{i+1}\sigma_{i+1}/k_i\sigma_i\mp k_{i+1}\times\sigma_{i+1}R_{i,i+1})\cdot\exp(\mp\sigma_{i+1}l_{i+1}),\quad n=1,2; \tag{3b}$$

$$u_{2n,i}=(1\mp k_{i+1}\sigma_{i+1}/k_i\sigma_i\mp k_{i+1}\times\sigma_{i+1}R_{i,i+1})\cdot\exp(\mp\sigma_{i+1}l_{i+1}),\quad n=1,2; \tag{3c}$$

$$\nu_{n1,i}=1\pm\beta_i/\sigma_i, n=1,2; \tag{3d}$$

$$\nu_{n2,i}=(-1\mp k_{i+1}\beta_{i+1}/k_i\sigma_i+k_{i+1}\times\beta_{i+1}R_{i,i+1})\cdot\exp(-\beta_{i+1}l_{i+1}); \tag{3e}$$

$$E_m=\frac{G_m}{\beta_m^2-\sigma_m^2}; \tag{4a}$$

$$G_m=\frac{\beta_m I_0}{2k_m}e^{-\sum_{i=m+1}^{N}\beta_i l_i}\ \text{ for }\ m<N, \tag{4b}$$

$$G_m=\frac{\beta_m I_0}{2k_m}\ \text{ for }\ m=N,\quad G_m=0,\quad \text{for }\ m=N+1.$$

In the above equations, $\sigma_i=(1+j)a_i$ with $j=\sqrt{-1}$ and $a_i=\sqrt{\pi f/\alpha_i}$. α_i is thermal diffusivity of layer i, f is the modulation frequency, k_i is the thermal conductivity of layer i, ρ is surface reflectivity of the sample, β_i is the optical absorption coefficient of layer i, and $R_{i,i+1}$ is thermal contact resistance between layer i and $i+1$. In the calculation, l_{N+1} is taken as 0 and $\Pi_{k=m}^{m-1}U_k$ is taken as $\left[\begin{smallmatrix}1 & 0\\ 0 & 1\end{smallmatrix}\right]$, where m is any integer between 0 and $N+1$.

The temperature in the gas layer is related to the phase shift and the amplitude of the PA signal. According to the generalized PA theory [23], the phase shift of the PA signal is calculated as $Arg(B_{N+1})-\pi/4$, and the amplitude is calculated as $Abs[(1-\rho)\cdot B_{N+1}P_0/\sqrt{2}l_{N+1}a_{N+1}T_0]$, where P_0 and T_0 are the ambient pressure and temperature, respectively.

III Experimental Details

The schematic of the experimental setup is shown in Fig. 1. A diode laser, which operates at a wavelength of 0.8 μm, is used as the heating source. The laser power driver is sinusoidally modulated by the internal function generator of a lock-in amplifier. The output power of the diode laser is around 150 mW at the modulation mode. After being reflected and focused, the laser beam is directed onto the sample mounted at the bottom of the PA cell. During the experiment, the maximum temperature rise at the sample surface is less than 0.5 °C. A condenser microphone, which is built into the PA cell, senses the acoustic signal and transfers it to the lock-in amplifier, where the amplitude and phase of the acoustic signal are measured. A personal computer, which is connected to the GPIB interface of the lock-in amplifier, is used for data acquisition and control of the experiment.

The PA cell used in this experiment is a cylindrical, small volume, resonance-free cell made of highly polished acrylic glass and a sapphire window. Both acrylic glass and sapphire have low reflection and high transmission for the laser beam used, so most of the laser energy reflected from the sample surface transmits out of the cell. At a frequency of 20 kHz, the wavelength of the acoustic wave is about 17.4 mm. In order to avoid resonance occurring in the cell, the characteristic cell size has to be less than 8.7 mm. Therefore, the cell is designed to have an axial bore of 4 mm in diameter and 6 mm high. The side of the bore facing the laser beam is sealed by the sapphire window, and the other side is sealed by the sample with an O-ring. In order to enhance the signal, the microphone is mounted 2 mm away from the inside wall of the cell, which is the smallest distance allowed by the size of the microphone and the cell. On the other hand, the smallest

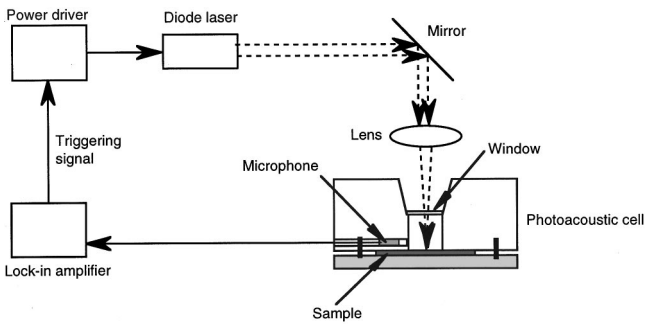

Fig. 1 Schematic diagram of the photoacoustic apparatus

size of the cell is limited by the dimension of the microphone. It is believed that the cell designed in this work is optimized considering both the signal to noise ratio enhancement and resonance suppression.

The PA response is delayed by the time for the acoustic wave to reach the microphone and the electronic circuitry. In order to remove the delay of the PA signal, reference samples of known thermal properties are used for calibration. Two reference samples are measured, one is a 3 mm thick graphite with its surface polished to 50 nm surface finishing, the other is a pure silicon wafer (0.381 mm thick) with a 70 nm thick nickel coating. Because of the small size of the laser beam (1 mm×2 mm), at frequencies lower than 2 kHz, the two-dimensional heat transfer effect could exist, hence, only frequencies from 2 kHz to 20 kHz are used. Within this frequency range, both the polished graphite and the Ni-Si are thick enough to be considered as bulk materials, and the phase shift is −90 deg. For the Ni-Si reference sample, the amplitude of the PA signal only depends on surface reflectivity and thermal properties of the silicon substrate.

After the phase shift of graphite, ϕ'_{graphite}, is obtained, the true phase shift of the sample, ϕ, is calculated as $\phi=\phi'-\phi'_{\text{graphite}}-90$, where ϕ' is the measured phase shift for the sample. The amplitude of the sample signal needs to be normalized with the reference signal since its absolute value is difficult to obtain. The normalized amplitude of the sample, A, is calculated as $A=A'/A'_{\text{Ni-Si}}\cdot A_{\text{Ni-Si}}$, where A' is the measured amplitude, $A'_{\text{Ni-Si}}$ is the measured amplitude for the Ni-Si reference sample, and $A_{\text{Ni-Si}}$ is the amplitude for the Ni-Si sample calculated using Eqs. (1)–(4).

The experimental setup is calibrated before each measurement. At each frequency, the signal is allowed to stabilize first, then data are taken every 8 sec. The phase shift and amplitude data are averaged every 5 min. A computer code determines whether the variation of the average phase shift over the five minutes time span is less than 0.2 deg, and the relative variation of the average amplitude is less than 0.5 percent. Data are stored when the above criterion is reached. In order to determine the drift of the signals with time, the references are also measured after each sample measurement.

A least square fitting procedure is used to determine unknown properties such as thermal conductivity and thermal contact resistance. Trial values of unknown properties are used to calculate the phase shift and the amplitude of the PA signal at each experimental frequency. For each trial value, the sum of the square of the difference between calculated values of phase shift and amplitude, and experimental ones is calculated. The trial values for which the least square is obtained are taken as the property values.

IV Results and Discussion

Thermal conductivities of thin SiO_2 films, nickel film, and thermal barrier coatings are measured. Results of the PA measurements will be first presented. Then, the measurement uncertainty of the PA technique will be discussed.

IV.1 Results of the PA Measurement

SiO_2 Films. Thermal conductivities of four SiO_2 films thermally grown on Si wafer are measured. The thicknesses of the SiO_2 films are 50, 101.9, 201.9 and 484.5 nm. In order to absorb the laser beam, a 70 nm thick nickel film is deposited on top of the SiO_2 layer by e-beam evaporation. The thickness of the nickel film is monitored during the evaporation process. The final film thickness is measured with an accuracy of 0.5 nm.

In Fig. 2, the phase shift as a function of the modulation frequency for the 484.5 nm thick SiO_2 sample is shown. The thermal conductivity of SiO_2 is fitted to be 1.71 W/m·K. Based on the ±0.2 deg uncertainty of the experiment, the uncertainty of thermal conductivity is found to be ±0.08 W/m·K. The fitting lines corresponding to the experimental uncertainty are also shown in Fig. 2. Figure 3 shows thermal conductivities of all the four SiO_2 films. From the figure, it is seen that thermal conductivities of all the SiO_2 films are around 1.66 W/m·K, higher than the thermal conductivity of fused silica (1.4 W/m·K). As shown in Fig. 3, variations of the thermal conductivity with thickness are not evident. This could indicate that the structure of the thermally grown SiO_2 film changes little with thickness.

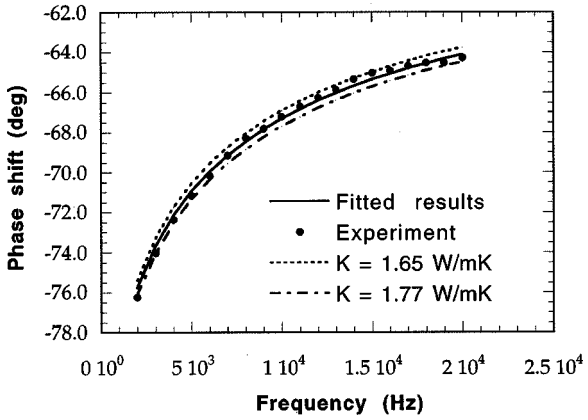

Fig. 2 Phase shift as a function of the modulation frequency of the 70 nm Ni—484.5 nm SiO_2—Si sample

Thermal conductivities of SiO_2 are also obtained by fitting the amplitude of the PA signal. Since the same 70 nm Ni layer is coated on the Ni-Si reference and the samples, reflectivity is expected to be the same, which is verified by measurements. Figure 4 illustrates the normalized amplitude for the 484.5 nm thick SiO_2 sample. The thermal conductivity is found to be 1.47 W/m·K. Based on the ±0.5 percent experimental uncertainty of the measured amplitude of PA signal, the numerical uncertainty analysis shows that the thermal conductivity has an uncertainty of about ±0.1 W/m·K. Thermal conductivity data of SiO_2 with different thicknesses obtained by amplitude fitting are summarized in Fig. 5. From this figure, it seems that thermal conductivity of SiO_2 slightly decreases with the thickness increase, which is not seen in the results obtained from phase shift fitting. However, this trend is not conclusive due to the experimental uncertainties of the measured amplitude of the PA signal. For thinner films, the signal is weaker and less stable, therefore the signal has a larger uncertainty of about ±1.5 percent, which causes a larger uncertainty in the final fitted results. Also when the film thickness is much less than the thermal diffusion length, for the same experimental un-

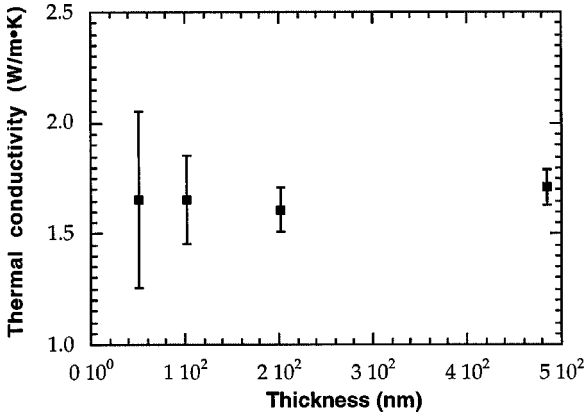

Fig. 3 Thermal conductivity of SiO_2 films obtained by phase shift fitting

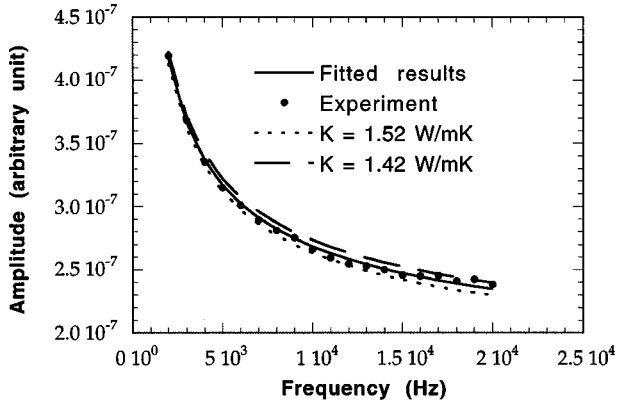

Fig. 4 Normalized amplitude as a function of the modulation frequency of the 70 nm Ni—484.5 nm SiO_2—Si sample

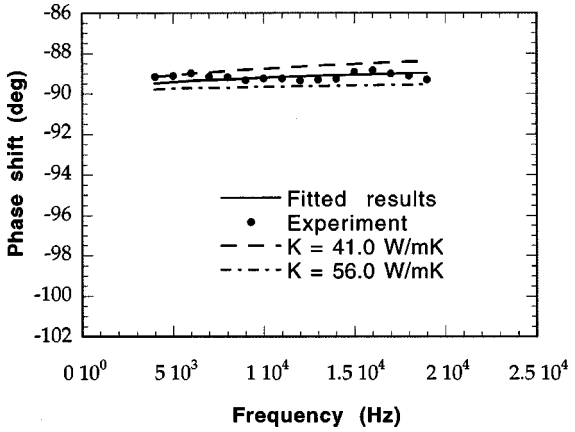

Fig. 6 Phase shift as a function of the modulation frequency of the 999.5 nm Ni—Si sample

certainty, the thinner film will have a larger uncertainty for its fitted thermal conductivity. The measurement sensitivity is discussed in more detail in IV.2.

From Fig. 3 and Fig. 5, it is seen that there is some discrepancy between the thermal conductivity measured by phase shift fitting and amplitude fitting. This discrepancy mostly comes from the uncertainty in the reflectivity measurement, which is required for amplitude fitting, but not for phase shift fitting. If the calculation includes the effect of the uncertainty in the reflectivity measurement, the uncertainty of the thermal conductivity resulted from amplitude fitting will be larger, on the order of 15 percent for the 484.5 nm thick SiO_2 film and 25 percent for the 50 nm-thick SiO_2 film. The thermal conductivity of the SiO_2 film measured in this work is slightly larger than that of fused silica ($k=1.4$ W/m·K). For thermally grown thin SiO_2 films, measurements using other techniques also showed similar results [7], which were explained as a higher level of crystallinity in SiO_2 thin films than in fused silica.

From both phase shift and amplitude fitting, the thermal contact resistances between the nickel coating and the SiO_2 film, and between the SiO_2 film and the Si wafer, are found to be less than 10^{-8} K·m^2/W. When thermal contact resistances are less than 10^{-8} K·m^2/W, they do not affect the PA signals, and thus can not be determined. Larger thermal contact resistances were found in some other samples [23].

Nickel Film. A thin nickel film is deposited on a pure 0.381 mm thick Si wafer using e-beam evaporation. The thickness of the nickel film is 999.5 ± 0.5 nm. Reflectivity of the sample is measured to be 0.595. Figures 6 and 7 show the phase shift and the normalized amplitude, respectively. By fitting the phase shift data, the thermal conductivity of the nickel film is found to be 47.5 W/m·K, with an upper limit of 56.0 W/m·K and a lower limit of 41.0 W/m·K. Using amplitude fitting, the thermal conductivity of the nickel film is found to be 35.3 W/m·K. Based on the 1 percent reflectivity measurement error, the thermal conductivity has an upper limit of 54.2 W/m·K and a lower limit of 26.0 W/m·K. Therefore, the thermal conductivity of the nickel film prepared in this work is less than the bulk value of 90.7 W/m·K. The thermal contact resistance between the nickel coating and the Si wafer is also found to be less than 10^{-8} K·m^2/W.

Similar to the measurement of the SiO_2 films, the accuracy of determining thermal conductivity of the Ni film with amplitude fitting is influenced by uncertainties in both the amplitude measurement and the surface reflectivity measurement. Since reflectivity is not needed for phase shift fitting, the thermal conductivity obtained from amplitude fitting has a larger uncertainty range than that obtained from phase shift fitting.

Bulk Materials With Mirror-Like Surface. For bulk materials, the phase shift of the PA signal is -90 deg, no information can be extracted from phase shift fitting. Therefore, only amplitude fitting can be used to obtain thermal conductivity of bulk materials. To demonstrate the PA technique for measuring thermal conductivities of bulk materials, the thermal conductivity of a glass slide is measured. A 70 nm thick nickel coating is deposited onto the glass to absorb the laser beam. Calculations show that this thin nickel layer has no effect on determining the thermal conductivity of glass. The fitting results are shown in Fig. 8. Thermal conduc-

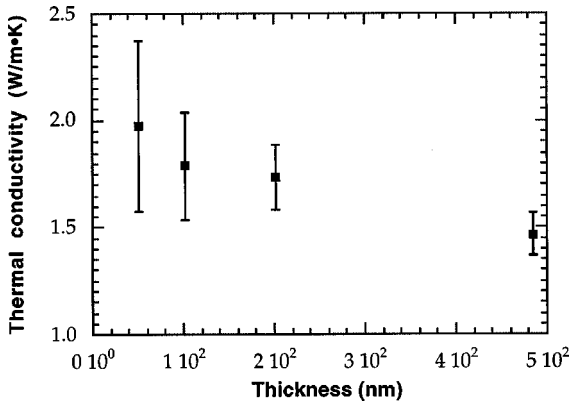

Fig. 5 Thermal conductivity of SiO_2 films obtained by amplitude fitting

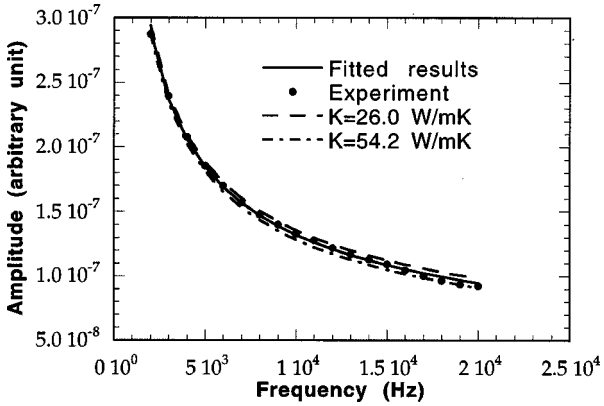

Fig. 7 Normalized amplitude as a function of the modulation frequency of the 999.5 nm Ni—Si sample

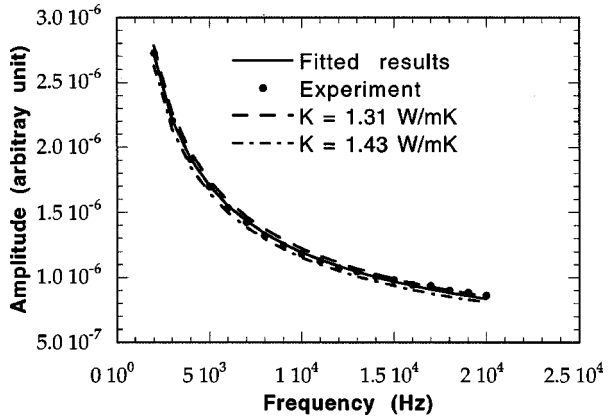

Fig. 8 Normalized amplitude as a function of the modulation frequency of the 70 nm Ni—glass sample

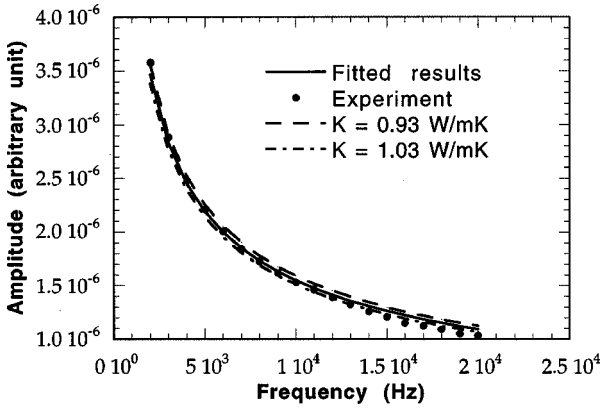

Fig. 10 Normalized amplitude as a function of the modulation frequency of Sample #1787

tivity of glass slide is found to be 1.38 W/m·K, with an upper limit of 1.43 W/m·K and a lower limit of 1.31 W/m·K. This result agrees with the literature value of 1.4 W/m·K [25].

Bulk Materials With Rough Surface. For bulk materials with mirror-like surfaces, measuring surface reflectivity is straightforward. For those with rough surfaces, an ellipsoid is used to measure the diffuse reflectivity. The apparatus is shown in Fig. 9. The sample is placed at one focal point, F1, of the ellipsoid and the detector is placed at the other focal point, F2. The diffusely reflected light from the sample surface is reflected by the inner wall of the ellipsoid and directed to the focal point F2, then is detected by the power meter. In the measurement, the sample is tilted by about 10 deg, so the specular reflection can reach the inner wall of the ellipsoid. Some diffusely reflected light, P_2, will be lost through the open aperture of the ellipsoid. This lost energy is estimated as $P_2 = P_1 * \Omega_2 / \Omega_1$ where P_1 is the energy measured by the detector, Ω_2 is the solid angle of the open aperture with respect to the sample, and Ω_1 is $(2\pi - \Omega_2)$. The variation of the directional reflectivity of the rough sample surface is found to be between 10~15 percent over the surface. Based on this, along with considering the 5 percent measurement error of the power meter, the error for the diffuse reflectivity measurement is estimated to be 10~15 percent.

Thermal conductivities of three thermal barrier coatings and its substrate material, all with rough surfaces are measured. Samples and sample numbers are provided by TPRL.[1] The normalized amplitude as a function of frequency for Sample #1787, which is a 68 μm thick thermal barrier coating on an alloy substrate, is shown in Fig. 10. Thermal conductivity is fitted to be 0.98 $\pm$0.05 W/m·K. The uncertainty of this thermal conductivity value mostly comes from the reflectivity measurement. Surface reflectivity and thermal conductivity values of all the thermal barrier coatings are summarized in Table 1. Sample #1897 is a copper based alloy used as the substrate of the thermal barrier coatings, and Sample #1736 and Sample #1758 are thermal barrier materials prepared by different techniques. The reference values are measured using a laser-flash method at TPRL, with an uncertainty of about $\pm$5 percent. It is seen that the thermal conductivity values obtained from the PA method are in close agreement with the data obtained from the laser-flash method. To reduce the uncertainty of the PA measurement, a more accurate diffuse reflectivity measurement method is required.

[1]Thermophysical Properties Research Laboratory Inc., West Lafayette, IN.

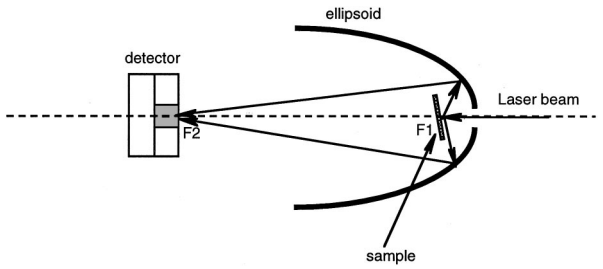

Fig. 9 Schematic diagram of the apparatus for measuring diffuse reflectivity

IV.2 Discussions. Using phase shift fitting, the photoacoustic technique is most suitable for measuring thin films whose thicknesses, l, are on the same order of the thermal diffusion depth, $l_\alpha (= \sqrt{\alpha/\pi f})$. Since the frequency f can be varied in a range, thermal properties of samples within a certain thickness range can be determined accurately. On the other hand, for thin films with thicknesses much less or larger than l_α, the measurement will be less accurate. Based on the results obtained in this work and the uncertainty of the phase shift measurement ($\pm$0.2 deg), the numerical uncertainty analysis indicates a $\pm$5 percent uncertainty of the thermal conductivity measurement when l_α / l is around 10 (e.g., the 484.5 nm SiO_2 sample). When l_α / l is around 100, the uncertainty of the thermal conductivity measurement is around $\pm$15 percent (e.g., the 50 nm SiO_2 sample). On the other hand, when the top layer is thick enough that l_α / l is less than 0.15 (e.g., the thermal barrier coatings), the modulated temperature field does not penetrate to the interface of the first two layers, thus, the top layer should be considered as a bulk material. In this case, its thermal conductivity cannot be obtained using phase shift fitting. These uncertainties are summarized in Table 2. Note that the above analysis only applies to the experiment with a $\pm$0.2 deg uncertainty. For an apparatus with a different measurement uncertainty, the uncertainties of the results need to be re-evaluated.

When the thermal conductivity is determined from amplitude fitting, the uncertainty of thermal conductivity is mostly determined by the uncertainty in the surface reflectivity measurement. Based on numerical sensitivity studies, the uncertainty of thermal

Table 1 Thermal conductivity of samples from TPRL

Sample index	Surface reflectivity	Thermal conductivity measured by the PA method (W/m·K)	Thermal conductivity measured by the laser flash method (W/m·K)
#1897	0.30 ± 10%	371 ± 32	333 ± 5%
#1736	0.10 ± 15%	0.45 ± 0.02	0.42 ± 5%
#1758	0.35 ± 10%	0.61 ± 0.07	0.66 ± 5%
#1787	0.15 ± 15%	0.98 ± 0.05	0.96 ± 5%

Table 2 Uncertainty of the thermal conductivity measurement (based on ±0.2 deg uncertainty of the measured phase shift, and ±5 percent uncertainty of the measured absorptivity)

l_α / l	Relative uncertainty of the thermal conductivity measurement	Example in this work
< 0.15	± 10% (Amplitude)	Thermal Barrier Coatings
10	± 5% (Phase shift)	484.5 nm SiO_2
100	± 15% (Phase shift)	50 nm SiO_2

conductivity is found to be about twice of that of the absorptivity measurement. Note that in Table 1, the measured surface reflectivity has a large uncertainty, on the order of 10 percent–15 percent. However, the uncertainty in absorptivity is much less, which results in a relatively accurate measurement of thermal conductivity that compares favorably with the results obtained by the laser flash method.

Comparing the PA method (amplitude fitting) with the laser flash method for measuring thermal conductivities of bulk materials, the advantage of the PA method is that it can measure thermal conductivities of coatings that can be treated as bulk materials. On the other hand, the amplitude fitting method has two limitations in comparison with the laser flash method. One is that reflectivity is required for the PA method. The other one is that the PA method works only at the room temperature. Technically, it is possible to develop a high temperature PA apparatus, with the highest temperature limited by the operation temperature of the transducer (normally around a few hundred degrees Celsius). The laser flash method, on the other hand, can measure thermal diffusivities above 1000 °C

Although all the film samples measured in this work do not have significant thermal contact resistance, the current PA apparatus does have the capability of measuring the thermal contact resistance. For example, for a sample of 1.03 μm-thick Ni on glass, the thermal contact resistance between the nickel film and the glass substrate is found to be $5.3 \pm 1.8 \times 10^{-7}$ m^{2}K/W [23]. For a film with thickness l and thermal conductivity k, its thermal resistance will be l/k. If the uncertainty of the thermal conductivity measurement is Δk, then the uncertainty in the thermal resistance is $l \cdot \Delta k/k^2$. Therefore, the smallest measurable thermal contact resistance at the interface of that layer is about $l \cdot \Delta k/k^2$, which corresponds to about 10^{-8} m^{2}K/W for the 484.5 nm SiO_2 film in this work. When the uncertainty in the thermal contact resistance is much larger than the thermal resistance of the film, the thermal contact resistance will play a major role in determining the PA signal. For a layer whose thermal contact resistance has an experimental uncertainty of ΔR, and whose thermal resistance is less than ΔR, the effect of thermal resistance will not be sensed by the experiment. Therefore, the largest measurable thermal conductivity of the layer is $l/\Delta R$.

V Conclusions

This work evaluated the PA technique for measuring thermal conductivities of thin films and bulk materials. In addition to commonly used phase shift fitting, an amplitude fitting method was also employed to determine thermal conductivities of thin films and bulk materials. Thermal conductivities of thin SiO_2 films thermally grown on Si wafer with different thicknesses were measured. It was found that the thermal conductivity of SiO_2 film changed little with thickness. The amplitude fitting method was used successfully to obtain thermal conductivities of bulk materials with smooth or rough surfaces. For bulk materials, thermal conductivity data obtained by the PA method were close to the literature values or the values obtained by the laser flash technique. It was demonstrated that the PA method could be used to determine thermal conductivities of a wide range of materials.

Acknowledgments

Support to this work by the National Science Foundation (CTS-9624890) is acknowledged. The authors would also like to thank Dr. Raymond Taylor of TPRL for providing thermal barrier coating samples, Dr. Magnus Rohde of the Institute of Materials Research at Karlsruhe, Germany for his help in the design of the PA cell, and David A. Willis and Jae Wook Ryu of the School of Mechanical Engineering, Purdue University for e-beam evaporation.

Nomenclature

a = $\sqrt{\pi f/\alpha}$
A = amplitude
B = intermediate coefficient
E, G = intermediate parameter
f = modulation frequency
I = intensity of laser light
j = imaginary unity
k = thermal conductivity
l = thickness
P = laser energy measured by power meter
R = thermal contact resistance
u = element of matrix U
v = element of matrix V
U, V = intermediate coefficient matrix

Greek Symbols

α = thermal diffusivity
β = optical absorption coefficient
ϕ = phase shift
θ = complex temperature
ρ = reflectivity
σ = $(1+j)a$
ω = modulated angular frequency
Ω = solid angle

Subscripts

i = layer i in the multi-layer system

References

[1] Goodson, K. E., and Flik, M. I., 1994, ''Solid Layer Thermal-Conductivity Measurement Techniques,'' Appl. Mech. Rev., **47**, pp. 101–112.
[2] Mirmira, S. R., and Fletcher, L. S., 1998, ''Review of the Thermal Conductivity of Thin Films,'' J. Thermophys. Heat Transfer, **12**, pp. 121–131.
[3] Völklein, F., 1990, ''Thermal Conductivity and Diffusivity of a Thin Film SiO_2-Si_3N_4 Sandwich System,'' Thin Solid Films, **188**, pp. 27–33.
[4] Cahill, D. G., 1990, ''Thermal Conductivity Measurement from 30 to 750 K: the 3ω Method,'' Rev. Sci. Instrum., **61**, pp. 802–808.
[5] Cahill, D. G., and Allen, T. H., 1994, ''Thermal Conductivity of Sputtered and Evaporated SiO_2 and TiO_2 Optical Coatings,'' Appl. Phys. Lett., **65**, pp. 309–311.
[6] Zhou, S. Q., Chen, G., Liu, J. L., Zheng, X. Y, and Wang, K. L., 1998, ''Anisotropic Thermal Conductivity of Si/SiGe Superlattice,'' *Proceedings of the 1998 ASME International Mechanical Engineering Congress and Exposition*, ASME, Fairfield, NJ, **361-4**, pp. 249–254.
[7] Okuda, M., and Ohkubo, S., 1992, ''A Novel Method for Measuring the Thermal Conductivity of Submicrometer Thick Dielectric Films,'' Thin Solid Films, **213**, pp. 176–181.
[8] Zhang, X., and Grigoropoulos, C. P., 1994, ''The Amplitude Technique for Measurement of Free Standing Thin Film Thermal Properties: a Comparison with other Experimental Techniques,'' *Proceedings of the 1994 ASME International Mechanical Engineering Congress and Exposition*, ASME, New York, NY, **293**, pp. 17–24.
[9] Goodson, K. E., Flik, M. I., Su, L. T., and Antoniadis, D. A., 1994, ''Prediction and Measurement of the Thermal Conductivity of Amorphous Dielectric Layers,'' ASME J. Heat Transfer, **116**, pp. 317–324.
[10] Goodson, K. E., Käding, O. W., Rösler, M., and Zachai, R., 1995, ''Experimental Investigation of Thermal Conduction Normal to Diamond-Silicon Boundaries,'' J. Appl. Phys., **77**, pp. 1385–1392.
[11] Wu, Z. L., Reichling, M., Hu, X. Q., Balasubramanian, K., and Guenther, K. H., 1993, ''Absorption and Thermal Conductivity of Oxide Thin Films Measured by Photothermal Displacement and Reflectance Methods,'' Appl. Opt., **32**, pp. 5660–5665.
[12] Machlab, H., McGahan, W. A., and Woollam, J. A., 1992, ''Thermal Diffusivity Measurements by Photothermal Laser Beam Deflection (PTD): Data

Analysis Using the Levenberg-Marquardt Algorithm,'' Thin Solid Films, **215**, pp. 103–107.
[13] Capinski, W. S., and Maris, H. J., 1996, ''Thermal Conductivity of GaAs/AlAs Superlattices,'' Physica B, **219 and 220**, pp. 699–701.
[14] Hostetler, J. L., Smith, A. N., and Norris, P. M., 1997, ''Thin-Film Thermal Conductivity and Thickness Measurements Using Picosecond Ultrasonics,'' Microscale Thermophys. Eng., **1**, pp. 237–244.
[15] Tam, A. C., 1986, ''Applications of Photoacoustic Sensing Techniques,'' Rev. Mod. Phys., **58**, pp. 381–431.
[16] Rosencwaig, A., and Gersho, A., 1976, ''Theory of the Photoacoustic Effect With Solids,'' J. Appl. Phys., **47**, pp. 64–69.
[17] Fujii, Y., Moritani, A., and Nakai, J., 1981, ''Photoacoustic Spectroscopy Theory for Multi-Layered Samples and Interference Effect,'' Jpn. J. Appl. Phys., **20**, pp. 361–367.
[18] Baumann, J., and Tilgner, R., 1985, ''Determining Photothermally the Thickness of a Buried Layer,'' J. Appl. Phys., **58**, pp. 1982–1985.
[19] Cole, K. D., and McGahan, W. A., 1992, ''Theory of Multilayers Heated by Laser Absorption,'' *Proceedings of Winter Annual Meeting of the American Society of Mechanical Engineering*, ASME, New York, NY, **40**, pp. 267–282.
[20] Lachaine, A., and Poulet, P., 1984, ''Photoacoustic Measurement of Thermal Properties of a Thin Polyester Film,'' Appl. Phys. Lett., **45**, pp. 953–954.
[21] Raman, S. S., Nampoori, V. P. N., Vallabhan, C. P. G., Ambadas, G., and Sugunan, S., 1995, ''Photoacoustic Study of the Effect of Degassing Temperature on Thermal Diffusivity of Hydroxyl Loaded Alumina,'' Appl. Phys. Lett., **67**, pp. 2939–2941.
[22] Rohde, M., 1994, ''Photoacoustic Characterization of Thermal Transport Properties in Thin Films and Microstructures,'' Thin Solid Films, **238**, pp. 199–206.
[23] Hu, H., Wang, X., and Xu, X., 1999, ''Generalized Theory of the Photoacoustic Effect with a Multilayer Material,'' J. Appl. Phys., **86**, pp. 3953–3958.
[24] Quimby, R. S., and Yen, W. M., 1980, ''On the Adequacy of One-Dimensional Treatments of the Photoacoustic Effect,'' J. Appl. Phys., **51**, pp. 1252–1253.
[25] Incropera, F. P., and DeWitt, D. P., 1990, *Fundamentals of Heat and Mass Transfer*, 3rd Ed., Wiley, New York, p. A13.